Search for $t\bar{t}$ resonances in semileptonic final states in pp collisions at $\sqrt{s} = 8$ TeV

Paul Turner on behalf of the CMS Collaboration

University of Illinois at Chicago

pturne7@uic.edu

DPF 2013 Meeting at UC Santa Cruz

August 15, 2013

Outline

1. Introduction
2. CMS Detector
3. Event Selection
4. $M_{t\bar{t}}$ Reconstruction
5. Monte Carlo Samples
6. Results
7. Statistical Analysis
8. Limits
9. Conclusions
10. Backup Slides

Search for $t\bar{t}$ resonances in semileptonic final states

P. Turner

Introduction

CMS Detector

Event Selection

$M_{t\bar{t}}$ Reconstruction

Monte Carlo Samples

Results

Statistical Analysis

Limits

Conclusions

Backup Slides

Introduction

- Several extensions to the standard model (SM) predict gauge interactions with enhanced couplings to the top quark.
- Massive new particles can manifest as resonances in the production of $t\bar{t}$ pairs at the Large Hadron Collider (LHC)
- Each result in a distorted $t\bar{t}$ invariant mass spectrum w.r.t. the SM expectation. **This allows for a model independent search for beyond standard model (BSM) physics by looking at the $t\bar{t}$ invariant mass!**

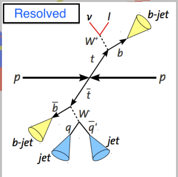

Introduction

- Several extensions to the standard model (SM) predict gauge interactions with enhanced couplings to the top quark.
- Massive new particles can manifest as resonances in the production of $t\bar{t}$ pairs at the Large Hadron Collider (LHC)

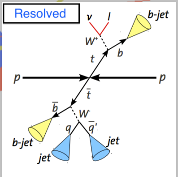

- Each result in a distorted $t\bar{t}$ invariant mass spectrum w.r.t. the SM expectation. **This allows for a model independent search for beyond standard model (BSM) physics by looking at the $t\bar{t}$ invariant mass!**

Introduction

- Several extensions to the standard model (SM) predict gauge interactions with enhanced couplings to the top quark.
- Massive new particles can manifest as resonances in the production of $t\bar{t}$ pairs at the Large Hadron Collider (LHC)
- Each result in a distorted $t\bar{t}$ invariant mass spectrum w.r.t. the SM expectation. **This allows for a model independent search for beyond standard model (BSM) physics by looking at the $t\bar{t}$ invariant mass!**

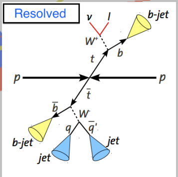

Introduction

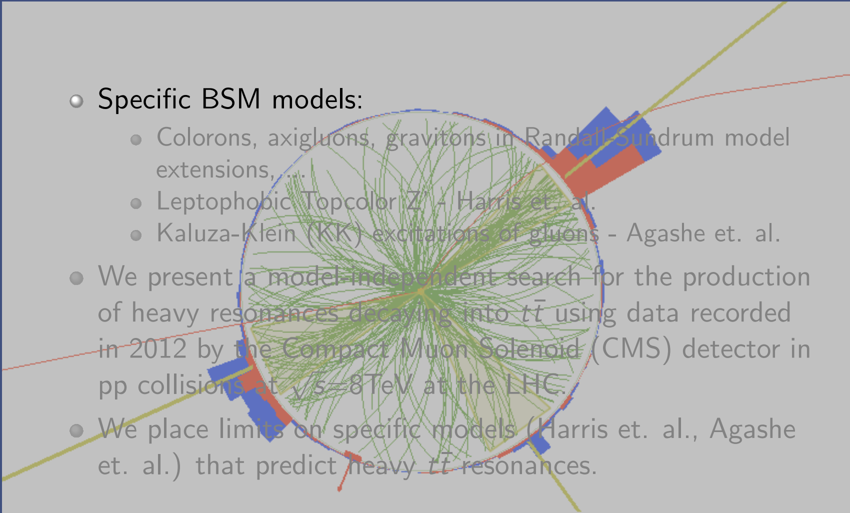

- Specific BSM models:
  - Colorons, axigluons, gravitons in Randall-Sundrum model extensions, ...
  - Leptophobic Topcolor Z' - Harris et. al.
  - Kaluza-Klein (KK) excitations of gluons - Agashe et. al.
- We present a model-independent search for the production of heavy resonances decaying into $t\bar{t}$ using data recorded in 2012 by the Compact Muon Solenoid (CMS) detector in pp collisions at $\sqrt{s}$=8TeV at the LHC.
- We place limits on specific models (Harris et. al., Agashe et. al.) that predict heavy $t\bar{t}$ resonances.

Introduction

- Specific BSM models:
  - Colorons, axigluons, gravitons in Randall-Sundrum model extensions, ...
  - Leptophobic Topcolor Z' - Harris et. al.
  - Kaluza-Klein (KK) excitations of gluons - Agashe et. al.
- We present a model-independent search for the production of heavy resonances decaying into $t\bar{t}$ using data recorded in 2012 by the Compact Muon Solenoid (CMS) detector in pp collisions at $\sqrt{s}$=8TeV at the LHC.
- We place limits on specific models (Harris et. al., Agashe et. al.) that predict heavy $t\bar{t}$ resonances.

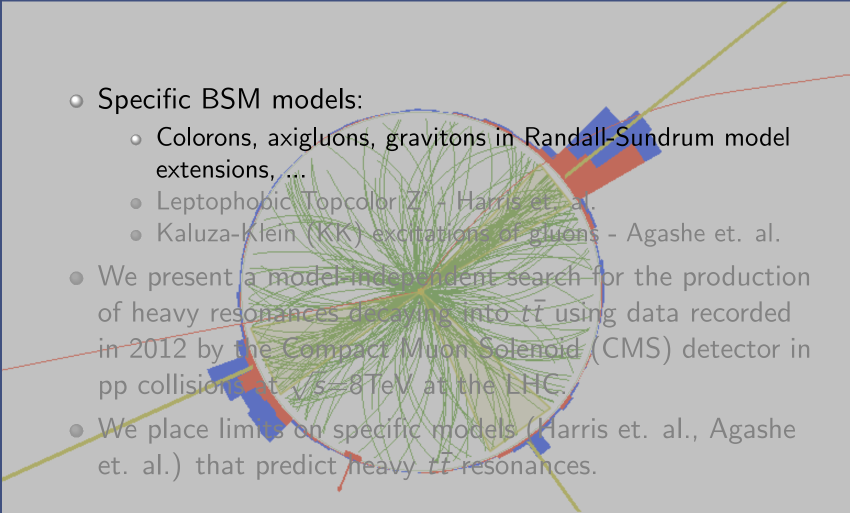

Introduction

- Specific BSM models:
  - Colorons, axigluons, gravitons in Randall-Sundrum model extensions, ...
  - Leptophobic Topcolor Z' - Harris et. al.
  - Kaluza-Klein (KK) excitations of gluons - Agashe et. al.
- We present a model-independent search for the production of heavy resonances decaying into $t\bar{t}$ using data recorded in 2012 by the Compact Muon Solenoid (CMS) detector in pp collisions at $\sqrt{s}$=8TeV at the LHC.
- We place limits on specific models (Harris et. al., Agashe et. al.) that predict heavy $t\bar{t}$ resonances.

Introduction

- Specific BSM models:
  - Colorons, axigluons, gravitons in Randall-Sundrum model extensions, ...
  - Leptophobic Topcolor Z' - Harris et. al.
  - Kaluza-Klein (KK) excitations of gluons - Agashe et. al.
- We present a model-independent search for the production of heavy resonances decaying into $t\bar{t}$ using data recorded in 2012 by the Compact Muon Solenoid (CMS) detector in pp collisions at $\sqrt{s}$=8TeV at the LHC.
- We place limits on specific models (Harris et. al., Agashe et. al.) that predict heavy $t\bar{t}$ resonances.

Introduction

- Specific BSM models:
    - Colorons, axigluons, gravitons in Randall-Sundrum model extensions, ...
    - Leptophobic Topcolor Z' - Harris et. al.
    - Kaluza-Klein (KK) excitations of gluons - Agashe et. al.
- We present a model-independent search for the production of heavy resonances decaying into $t\bar{t}$ using data recorded in 2012 by the Compact Muon Solenoid (CMS) detector in pp collisions at $\sqrt{s}$=8TeV at the LHC.
- We place limits on specific models (Harris et. al., Agashe et. al.) that predict heavy $t\bar{t}$ resonances.

Introduction

- Specific BSM models:
  - Colorons, axigluons, gravitons in Randall-Sundrum model extensions, ...
  - Leptophobic Topcolor Z' - Harris et. al.
  - Kaluza-Klein (KK) excitations of gluons - Agashe et. al.
- We present a model-independent search for the production of heavy resonances decaying into $t\bar{t}$ using data recorded in 2012 by the Compact Muon Solenoid (CMS) detector in pp collisions at $\sqrt{s}$=8TeV at the LHC.
- We place limits on specific models (Harris et. al., Agashe et. al.) that predict heavy $t\bar{t}$ resonances.

CMS Detector

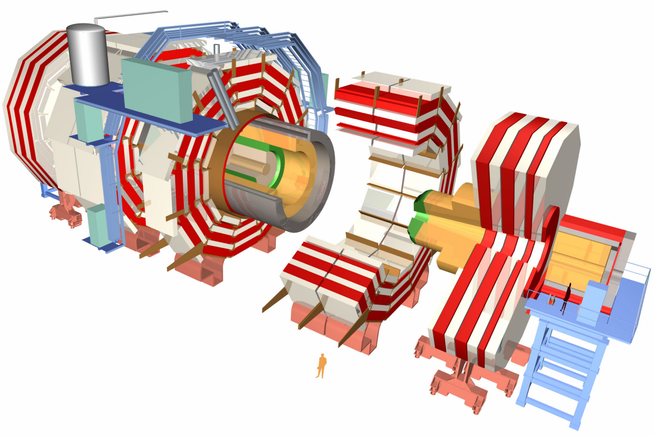

- Superconducting solenoid, 6m internal diameter, 3.8T
- Silicon Pixel and Strip Tracker
- Lead Tungstate Crystal Electromagnetic Calorimeter (ECAL)
- Brass/Scintillator hadron calorimeter (HCAL)
- Gas-ionization muon chambers are embedded in the steel return yoke of the solenoid
- Forward calorimetery complements the barrel and endcap detectors

Event Selection

Data consists of 19.6 fb^{-1} integrated luminosity of pp collisions at $\sqrt{s} = 8$ TeV collected by the CMS experiment in 2012.

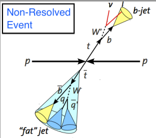

$\rightarrow$ Heavy resonance means boosted topology!

Electron Channel Trigger

-Electron w/$p_T > 30$GeV
-Jet w/$p_T > 100$GeV
-Jet w/$p_T > 25$GeV

Muon Channel Trigger

-Muon w/$p_T > 40$GeV

Event Selection

Data consists of 19.6 fb^{-1} integrated luminosity of pp collisions at $\sqrt{s} = 8$ TeV collected by the CMS experiment in 2012.

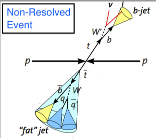

$\rightarrow$ Heavy resonance means boosted topology!

Electron Channel Trigger

-Electron w/$p_T > 30$GeV
-Jet w/$p_T > 100$GeV
-Jet w/$p_T > 25$GeV

Muon Channel Trigger

-Muon w/$p_T > 40$GeV

Event Selection

Data consists of 19.6 fb^{-1} integrated luminosity of pp collisions at $\sqrt{s} = 8$ TeV collected by the CMS experiment in 2012.

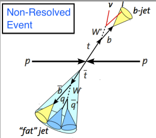

$\rightarrow$ Heavy resonance means boosted topology!

Electron Channel Trigger

-Electron w/$p_T > 30$GeV
-Jet w/$p_T > 100$GeV
-Jet w/$p_T > 25$GeV

Muon Channel Trigger

-Muon w/$p_T > 40$GeV

Event Selection

Data consists of 19.6 fb^{-1} integrated luminosity of pp collisions at $\sqrt{s} = 8$ TeV collected by the CMS experiment in 2012.

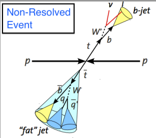

$\rightarrow$ Heavy resonance means boosted topology!

Electron Channel Trigger

-Electron w/$p_T > 30$GeV
-Jet w/$p_T > 100$GeV
-Jet w/$p_T > 25$GeV

Muon Channel Trigger

-Muon w/$p_T > 40$GeV

Offline Selection

- One electron(muon) w/p_T >35 GeV(45 GeV), $|\eta| < 2.5$ (2.1)
  - No isolation requirement!
- Veto on second lepton
- At least two jets $|\eta| < 2.4$
  - Leading jet $p_T > 150$ GeV, other jets $p_T > 50$ GeV
- $H_T^{lep} = E_T^{miss} + p_T^{lep} > 150$ GeV (Scalar)
- $E_T^{miss} > 50$ GeV

Offline Selection

- One electron(muon) w/p_T >35 GeV(45 GeV), $|\eta| < 2.5$ (2.1)
  - No isolation requirement!
- Veto on second lepton
- At least two jets $|\eta| < 2.4$
  - Leading jet $p_T > 150$ GeV, other jets $p_T > 50$ GeV
- $H_T^{lep} = E_T^{miss} + p_T^{lep} > 150$ GeV (Scalar)
- $E_T^{miss} > 50$ GeV

Offline Selection

- One electron(muon) w/p_T >35 GeV(45 GeV), $|\eta| < 2.5$ (2.1)
  - No isolation requirement!
- Veto on second lepton
- At least two jets $|\eta| < 2.4$
  - Leading jet $p_T > 150$ GeV, other jets $p_T > 50$ GeV
- $H_T^{lep} = E_T^{miss} + p_T^{lep} > 150$ GeV (Scalar)
- $E_T^{miss} > 50$ GeV

Offline Selection

- One electron(muon) w/p_T >35 GeV(45 GeV), $|\eta| < 2.5$ (2.1)
  - No isolation requirement!
- Veto on second lepton
- At least two jets $|\eta| < 2.4$
  - Leading jet $p_T > 150$ GeV, other jets $p_T > 50$ GeV
- $H_T^{lep} = E_T^{miss} + p_T^{lep} > 150$ GeV (Scalar)
- $E_T^{miss} > 50$ GeV

Offline Selection

Search for $t\bar{t}$ resonances in semileptonic final states

P. Turner

- One electron(muon) w/p_T >35 GeV(45 GeV), $|\eta| < 2.5$ (2.1)
  - No isolation requirement!
- Veto on second lepton
- At least two jets $|\eta| < 2.4$
  - Leading jet $p_T > 150$ GeV, other jets $p_T > 50$ GeV
- $H_T^{lep} = E_T^{miss} + p_T^{lep} > 150$ GeV (Scalar)
- $E_T^{miss} > 50$ GeV

Offline Selection

- 2D Cut : $\Delta R(lep, closestjet) > 0.5$ or $p_{T,rel}(lep, closestjet) > 25 GeV$

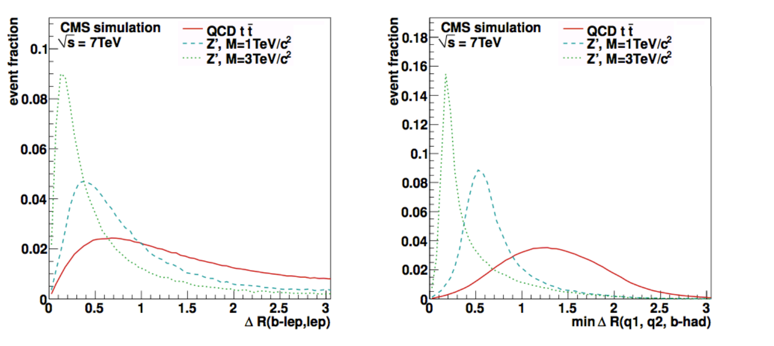

→ Do not cut hard on lepton isolation!

Offline Selection

- Triangular (topological) cut (removes events when E_T^{miss} opposite to electron or jet)

$$-\frac{1.5}{75GeV}E_T^{miss} + 1.5 < \Delta\Phi\{\text{ (e or j)}, E_T^{miss}\ \} < \frac{1.5}{75GeV}E_T^{miss} + 1.5$$

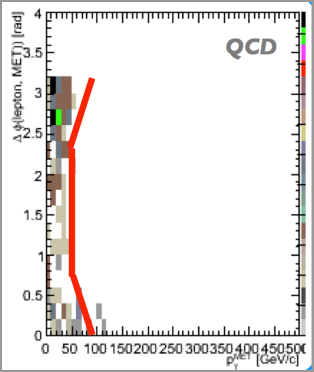

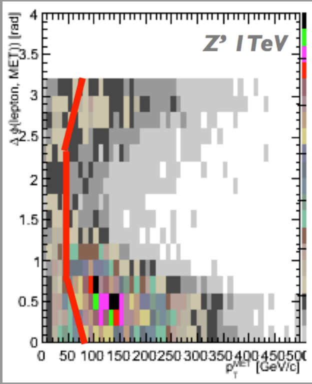

Event Selection

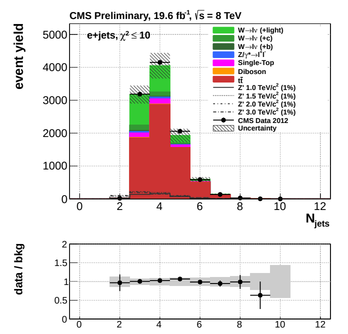

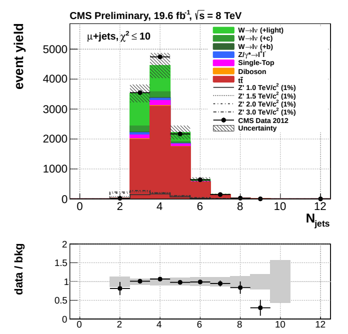

Number of jets distribution in the electron (muon) channel of the high-mass analysis.

Event Selection

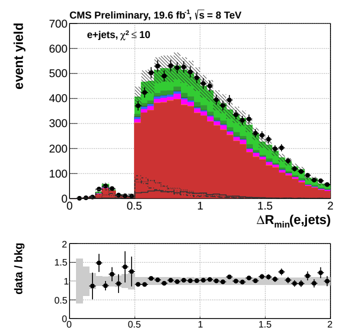

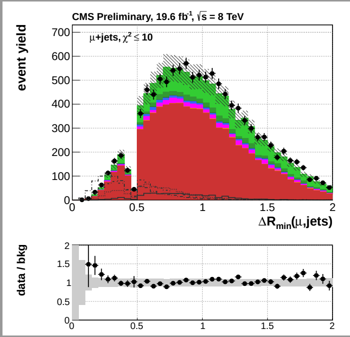

Distance ΔR between the electron(muon) and the closest jet.

2D Cut : ΔR (lepton, closest jet) > 0.5
or $p_{T,rel}$ (lepton, closest jet) > 25 GeV

Event Candidate

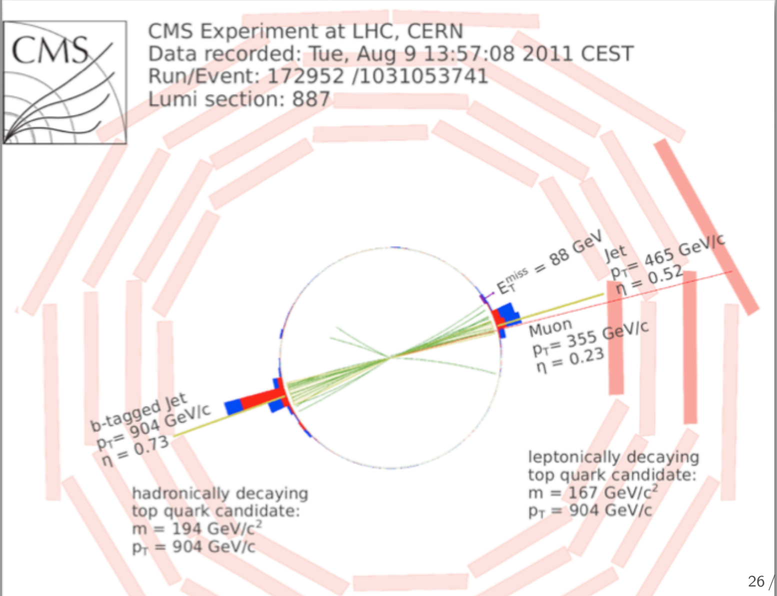

$M_{t\bar{t}}$ Reconstruction

- Each candidate has a list of jets, lepton, and E_T^{miss}(neutrino)
- t_{had} reconstructed with at least one jet
- t_{lep} reconstructed with at least one jet, E_T^{miss}, and one lepton
- Permute jet assignments to generate hypotheses

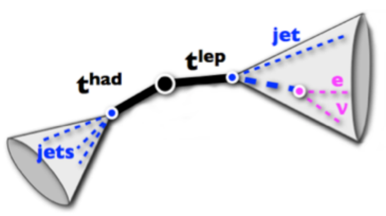

$M_{t\bar{t}}$ Reconstruction

- Each candidate has a list of jets, lepton, and E_T^{miss}(neutrino)
- t_{had} reconstructed with at least one jet
- t_{lep} reconstructed with at least one jet, E_T^{miss}, and one lepton
- Permute jet assignments to generate hypotheses

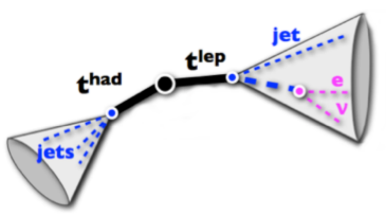

$M_{t\bar{t}}$ Reconstruction

- Each candidate has a list of jets, lepton, and E_T^{miss}(neutrino)
- t_{had} reconstructed with at least one jet
- t_{lep} reconstructed with at least one jet, E_T^{miss}, and one lepton
- Permute jet assignments to generate hypotheses

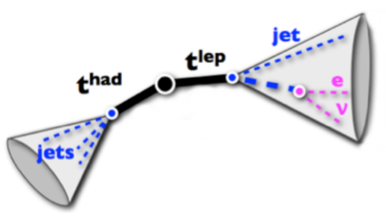

$M_{t\bar{t}}$ Reconstruction

- Each candidate has a list of jets, lepton, and E_T^{miss}(neutrino)
- t_{had} reconstructed with at least one jet
- t_{lep} reconstructed with at least one jet, E_T^{miss}, and one lepton
- Permute jet assignments to generate hypotheses

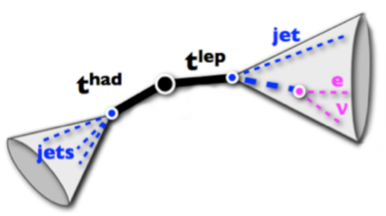

χ^2 Cut

- Select hypothesis with minimal χ^2, Cut on $\chi^2 < 10$
  - $\chi^2 = \chi^2_{lep} + \chi^2_{had}$

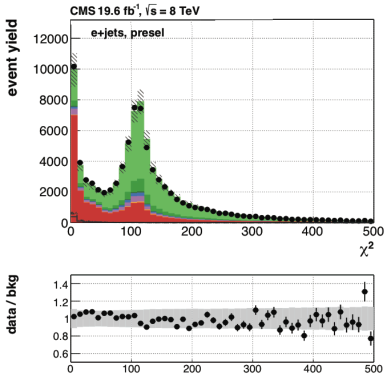

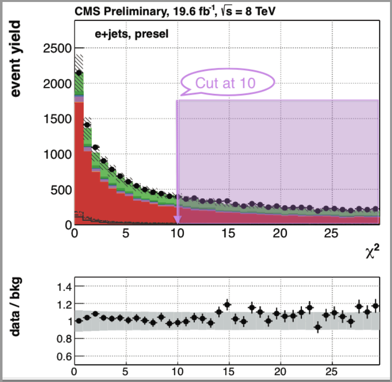

Top Jet Candidate

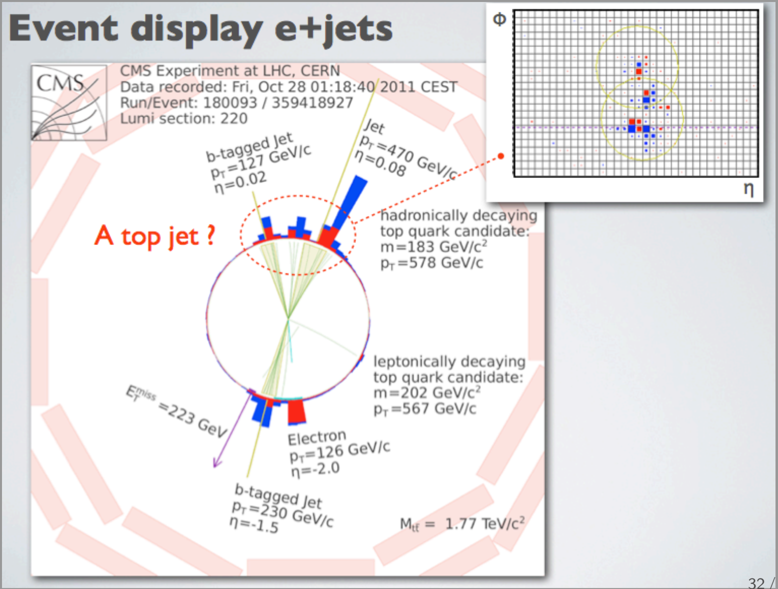

Selection Summary

$\rightarrow$ Increase the acceptance for our signal by allowing events with low jet multiplicity and non-isolated leptons. This causes the number of qcd events to dominate.

$\rightarrow$ Introduce two alternative cuts: 2D and triangular. This controls QCD.

$\rightarrow$ χ^2 cut controls W+jets

$\rightarrow$ Events are separated based on b-tagging. The aim is to have complementary channels with different W+jets/$t\bar{t}$ relative contributions.

Selection Summary

$\rightarrow$ Increase the acceptance for our signal by allowing events with low jet multiplicity and non-isolated leptons. This causes the number of qcd events to dominate.

$\rightarrow$ Introduce two alternative cuts: 2D and triangular. This controls QCD.

$\rightarrow$ χ^2 cut controls W+jets

$\rightarrow$ Events are separated based on b-tagging. The aim is to have complementary channels with different W+jets/$t\bar{t}$ relative contributions.

Selection Summary

$\rightarrow$ Increase the acceptance for our signal by allowing events with low jet multiplicity and non-isolated leptons. This causes the number of qcd events to dominate.

$\rightarrow$ Introduce two alternative cuts: 2D and triangular. This controls QCD.

$\rightarrow$ χ^2 cut controls W+jets

$\rightarrow$ Events are separated based on b-tagging. The aim is to have complementary channels with different W+jets/$t\bar{t}$ relative contributions.

Selection Summary

$\rightarrow$ Increase the acceptance for our signal by allowing events with low jet multiplicity and non-isolated leptons. This causes the number of qcd events to dominate.

$\rightarrow$ Introduce two alternative cuts: 2D and triangular. This controls QCD.

$\rightarrow$ χ^2 cut controls W+jets

$\rightarrow$ Events are separated based on b-tagging. The aim is to have complementary channels with different W+jets/$t\bar{t}$ relative contributions.

Monte Carlo Samples

- MadGraph-pythia combination is used to generate high-mass resonances with $\Gamma/m = 0.01$ and $\Gamma/m = 0.10$, where Γ is the width of the resonance, m=0.5,0.75,1,1.25,1.5,2, and 3 TeV resonance mass
- pythia 8 is used to generate a KK gluon excitation
- pythia and MadGraph used to generate backgrounds
- All samples include in-time and out-of-time pileup, re-weighted to reflect actual pileup conditions determined from data

Monte Carlo Samples

- MADGRAPH-PYTHIA combination is used to generate high-mass resonances with $\Gamma/m = 0.01$ and $\Gamma/m = 0.10$, where Γ is the width of the resonance, m=0.5,0.75,1,1.25,1.5,2, and 3 TeV resonance mass
- PYTHIA 8 is used to generate a KK gluon excitation
- PYTHIA and MADGRAPH used to generate backgrounds
- All samples include in-time and out-of-time pileup, re-weighted to reflect actual pileup conditions determined from data

Monte Carlo Samples

- MADGRAPH-PYTHIA combination is used to generate high-mass resonances with $\Gamma/m = 0.01$ and $\Gamma/m = 0.10$, where Γ is the width of the resonance, m=0.5,0.75,1,1.25,1.5,2, and 3 TeV resonance mass
- PYTHIA 8 is used to generate a KK gluon excitation
- PYTHIA and MADGRAPH used to generate backgrounds
- All samples include in-time and out-of-time pileup, re-weighted to reflect actual pileup conditions determined from data

Cross-Sections

Process	σ [pb]	Order	Generator
$t\bar{t}$	234	approx. NNLO	POWHEG
W+jet	37509	NNLO	MadGraph
WW	54.8	NLO	PYTHIA 6
WZ	33.2	NLO	PYTHIA 6
ZZ	8.059	NLO	PYTHIA 6
Z+jets	3504	NNLO	MadGraph
Single t, s-channel	3.79	approx. NNLO	POWHEG
Single $\bar{t}$, s-channel	1.76	approx. NNLO	POWHEG
Single t, t-channel	56.4	approx. NNLO	POWHEG
Single $\bar{t}$, t-channel	30.7	approx. NNLO	POWHEG
Single t, tW production	11.1	approx. NNLO	POWHEG
Single $\bar{t}$, tW production	11.1	approx. NNLO	POWHEG

Number of Events

Sample	Electron+Jets Channel $N_{b-tag} = 0$	Electron+Jets Channel $N_{b-tag} 1$	Muon+Jets Channel $N_{b-tag} = 0$	Muon+Jets Channel $N_{b-tag} 1$
Z', M=0.5TeV/c^2 (1%)	5.6	9.7	5.1	8.9
Z', M=0.75TeV/c^2 (1%)	50.7	108	59.2	114
Z', M=1TeV/c^2 (1%)	134.9	246.1	145	247.1
Z', M=1.25TeV/c^2 (1%)	211.3	319.4	222	321.6
Z', M=1.5TeV/c^2 (1%)	287.2	322.4	324.1	343.3
Z', M=2TeV/c^2 (1%)	355.4	300.3	497.8	318.7
Z', M=3TeV/c^2 (1%)	362.9	199.4	609.2	251.4
Z', M=0.5TeV/c^2 (10%)	7.6	11.3	6.4	14.1
Z', M=0.75TeV/c^2 (10%)	51.9	112.3	53.2	101.6
Z', M=1TeV/c^2 (10%)	118.5	216.8	133.4	230.7
Z', M=1.25TeV/c^2 (10%)	187.2	285.9	210.2	300.2
Z', M=1.5TeV/c^2 (10%)	261.2	290.5	287.8	323.8
Z', M=2TeV/c^2 (10%)	298.9	268.5	408.9	298.9
Z', M=3TeV/c^2 (10%)	243.9	218.6	356.2	231.1
g_{KK}, M=1TeV/c^2	101.9	163.4	119.8	118
g_{KK}, M=1.5TeV/c^2	178.3	215.1	217.8	250.6
g_{KK}, M=2TeV/c^2	202	195.6	281.7	224
g_{KK}, M=3TeV/c^2	151.6	154.7	224.2	174.1
Diboson	29.3	3.3	43.1	4.9
Single Top	266.6	384.5	284.4	418.2
$t\bar{t}$	2583.8	4372.9	2854.5	4718.5
W+jets(+b)	25.7	35.8	21.5	34.6
W+jets(+c)	319.8	23.2	421.1	37.4
W+jets(+light)	1985.5	49.6	2282	62.4
Z+jets	76.3	5.9	121.3	9.6
Total Background	5287±703	4875±658	6028±741	5285±629
Data 2012	5346	4820	5959	5339

Invariant Mass Distributions

Muon Channel:

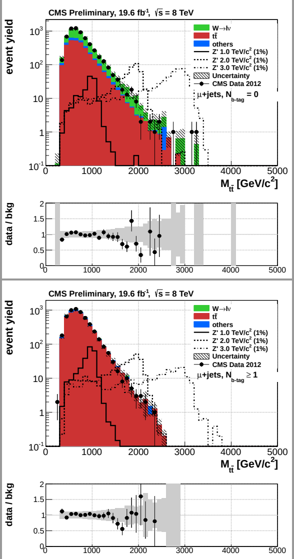

Electron Channel:

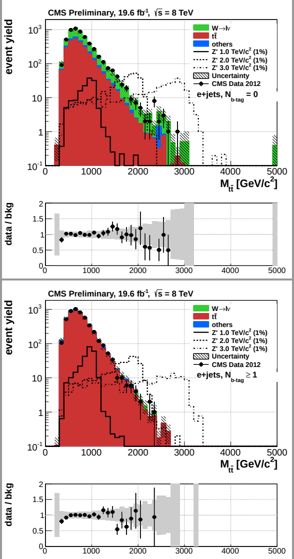

Statistical Analysis

- Statistical analysis is defined by using a bin likelihood of the invariant mass of the reconstructed $t\bar{t}$ system

$$L(\beta|data) = \prod_{i=1}^{N_{bins}} \frac{\mu_i^{n_i} e^{-\mu_i}}{n_i!}$$

$$\mu_i = \sum_k \beta_k T_{k,i}$$

- $T_{k,i}$ is the i-bin content for k-template.
- Lognormal distributions are used as prior for all the systematic uncertainties.

Summary of Systematic Uncertainties

Source of systematic uncertainty	Uncertainty	Type
ttbar cross section	15%	Normalization
electron trigger and id	5%	Normalization
Single top cross section	50%	Normalization
W_{light} +jets cross section	50%	Normalization
W_{heavy} +jets cross section	100%	Normalization
Z+jets cross section	100%	Normalization
Luminosity	4.4%	Normalization
muon trigger and id	$\pm 1\sigma(\eta)$	Normalization & Shape
Jet Energy Scale	$\pm 1\sigma(p_T, \eta)$	Normalization & Shape
Jet Energy Resolution	$\pm 1\sigma(\eta)$	Normalization & Shape
b-tagging	$\pm 1\sigma(p_T, \eta)$	Normalization & Shape
Mistag Rate	$\pm 1\sigma(p_T, \eta)$	Normalization & Shape
Pileup	$\pm 1\sigma$	Normalization & Shape
PDFs	CTEQ6 (CT10) set	Normalization & Shape
Scale ($Q^2 = M(t)^2 + \Sigma p_T(jet)^2$) for $t\bar{t}$	$2Q^2$ and $0.5Q^2$	Normalization & Shape
Scale ($Q^2 = M(t)^2 + \Sigma p_T(jet)^2$) for W/Z+jets	$2Q^2$ and $0.5Q^2$	Normalization & Shape
Matching for W/Z+jets	2 and 0.5 x default	Normalization & Shape

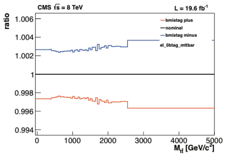

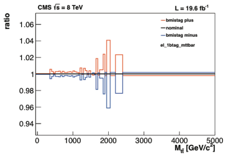

Cross Section

Bayesian statistical method used to extract 95% C.L. upper limits on Z' $\rightarrow t\bar{t}$ cross-section

Expected limits given by background-only pseudo-experiments ($\mu = 0$). Expected limit is given by the median of the distribution of upper limits, 68% and 95% give the $\pm$ 1 and $\pm$ 2 standard deviations.

Limits are calculated for threshold and boosted analysis separately, then combined where the transition between threshold and boosted is based on the expected sensitivity.

Limits (Narrow Resonances)

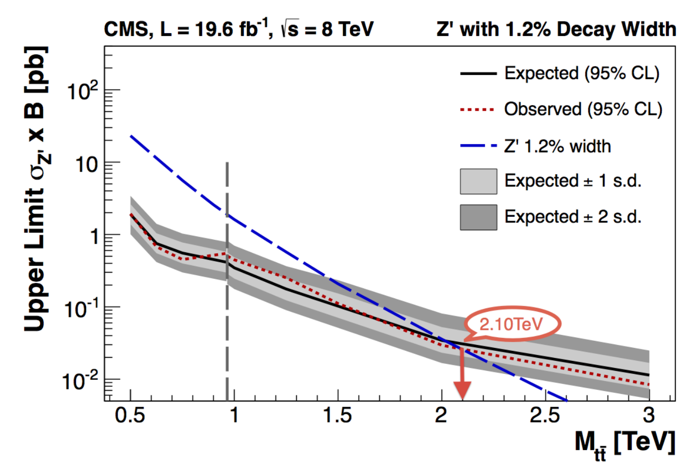

The 95% CL upper limits for narrow resonances. Theoretical prediction Harris et. al.

Limits (Wide Resonances)

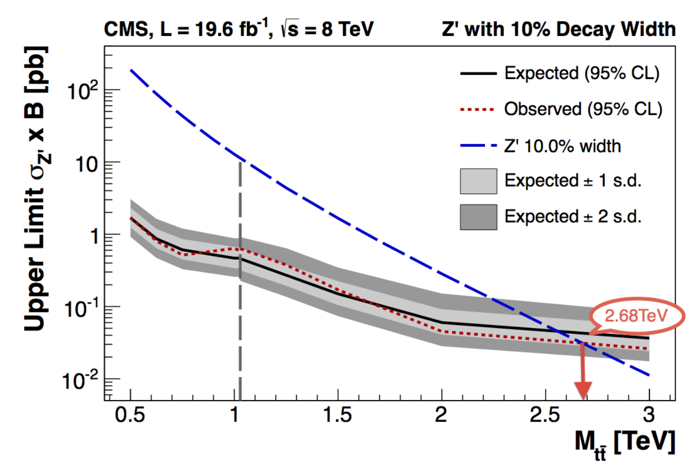

The 95% CL upper limits for resonances with 10% width.
Theoretical prediction Harris et. al.

Limits (KK Resonances)

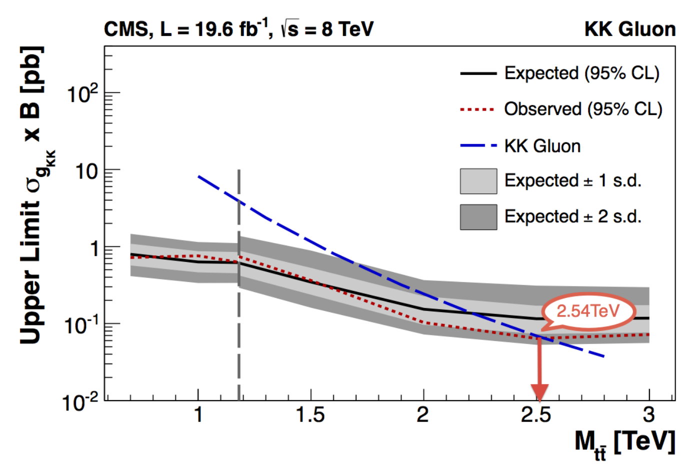

The 95% CL upper limits for Kaluza-Klein excitations of the gluon. Theoretical prediction Agashe et. al.

Conclusions

- We have presented a model-independent search for the production of heavy resonances decaying into $t\bar{t}$
- We have combined the results of two complementary analyses optimized for the threshold and boosted regions
- No evidence for a massive resonance is found, therefore we set model-independent limits on the production cross section of non-SM particles decaying to $t\bar{t}$

	0.5 TeV		2 TeV	
	Expected	Observed	Expected	Observed
Narrow	$1.91^{+0.76}_{-0.53}$ pb	1.94 pb	$0.034^{+0.018}_{-0.011}$ pb	0.029 pb
Wide	$1.69^{+0.67}_{-0.45}$ pb	1.71 pb	$0.060^{+0.032}_{-0.019}$ pb	0.045 pb

Conclusions

- In addition, we set the following limits at 95% C.L. on the production of non-SM particles in specific models.
  - Topcolor Z' bosons with a width of 1.2 and 10% are excluded at 95% C.L. for masses below 2.10 TeV and 2.68 TeV.
  - Kaluza-Klein excitations of a gluon with masses below 2.54 TeV in the Randall-Sundrum model are excluded and an upper limit of 0.101 pb ($0.150^{+0.072}_{-0.055}$ pb expected) is set on the production cross section times branching fraction for resonance of 2 TeV.
- Compared to the results of previous analyses, the upper limits on the masses of these specific resonances have been improved by several hundred GeV.

References

The CMS Collaboration (2013)
Search for $t\bar{t}$ resonances in semileptonic final states in pp collisions at $\sqrt{s} = 8$ TeV
CMS PAS B2G-12-006 Available on the CERN CDS information server

R. M. Harris and S. Jain
Cross Sections for Leptophobic Topcolor Z decaying to top-antitop
Eur. Phys. J. C 72 (2012) 2072 doi:10.1140/epjc/s10052-012-2072-4, arXiv:hep-ph/1112.4928

K. Agashe et al.
LHC Signals from Warped Extra Dimensions
Phys. Rev. D 77 (2008) 015003 doi:10.1103/PhysRevD.77.015003, arXiv:hep-ph/0612015

The End

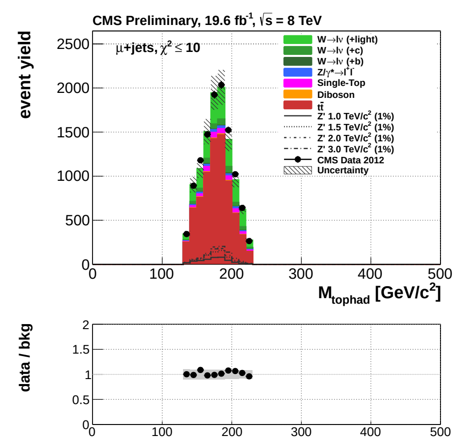

Figure : Distribution of the reconstructed mass of the leptonically decaying top quark in the muon channel of the high-mass analysis.

Backup Slides

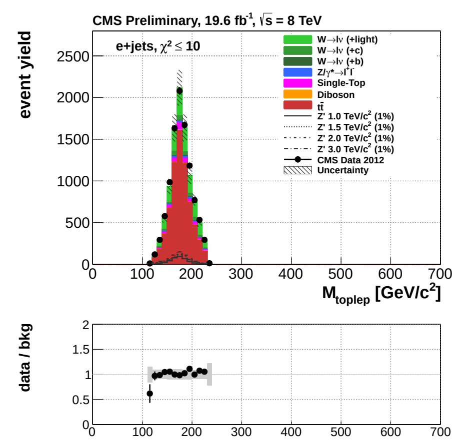

Figure : Distribution of the reconstructed mass of the leptonically decaying top quark in the electron channel of the high-mass analysis.

Backup Slides

Search for $t\bar{t}$ resonances in semileptonic final states

P. Turner

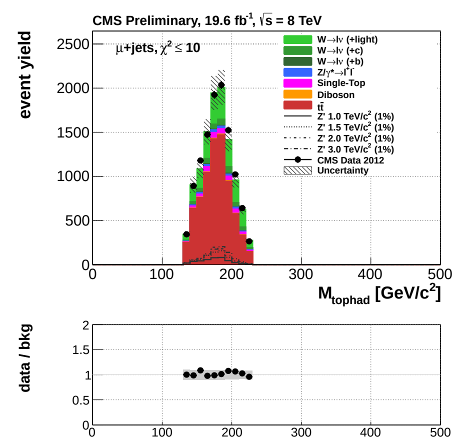

Figure : Distribution of the reconstructed mass of the hadronically decaying top quark in the muon channel of the high-mass analysis.

Backup Slides

Search for $t\bar{t}$ resonances in semileptonic final states

P. Turner

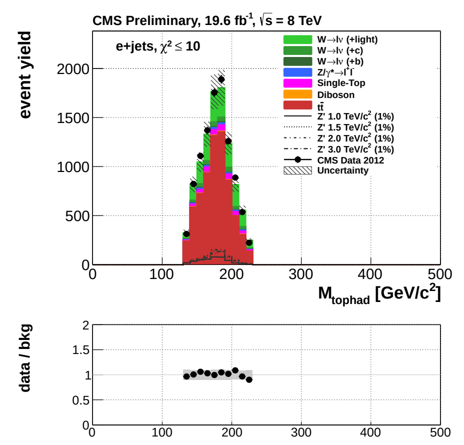

Figure : Distribution of the reconstructed mass of the hadronically decaying top quark in the electron channel of the high-mass analysis.